

Spin fluctuation theory for the insulating ground state of YbB_{12}

S. H. Liu

Department of Physics, University of California, San Diego, La Jolla, California 92093-03219

(Received 11 July 2000; revised manuscript received 31 October 2000; published 28 February 2001)

It is proposed that the insulating ground state of the compound YbB_{12} originates from a localized superposition of f^{14} and $f^{13}d^1$ configurations of Yb in a singlet spin state. The theory is formally similar to the well-known spin-fluctuation mechanism for magnetic impurities in metals. It explains both the insulating ground state and the band of dispersive excited states recently observed by neutron scattering. By making a few reasonable approximations for finite temperatures and spin-orbit coupling effects, we obtain a phenomenological model for the bulk properties that explains the temperature dependence of the specific heat, the susceptibility, and the inelastic neutron scattering line shape for powder samples.

DOI: 10.1103/PhysRevB.63.115108

PACS number(s): 71.28.+d, 71.27.+a, 75.30.Mb, 71.70.Ch

I. INTRODUCTION

The compound YbB_{12} belongs to a class of materials known as Kondo insulators. These are insulating compounds of Ce, Sm, or Yb, with energy gaps of the order of 100–200 K. Like that of other members of the family, the specific heat of YbB_{12} has the Schottky form whose peak falls around 50 K.^{1,2} The magnetic susceptibility rises three fold between helium temperature and a peak at 80 K, then declines slowly at higher temperatures. The high temperature behavior is reminiscent of the Curie-Weiss susceptibility of local moment systems. It appears that at lower temperatures the moments gradually disappear, in analogy with spin compensation or the Kondo effect for some magnetic impurities in metals. It is therefore believed that the opening of an energy gap in the electron spectrum in these insulators is a consequence of spin compensation. All attempts to explain the properties of this and other related materials are based on this line of reasoning.³ To summarize very briefly, the theory shows that in a metal the presence of a Ce or Yb impurity produces a spin-fluctuation resonance near the Fermi level.^{4,5} Hybridization of this level with the underlying d band leads to a pair of narrow bands separated by a gap.^{6,7} This gap is identified as the insulating gap.^{3,8} The theory implies that the formation of the energy gap is possible only in a periodic lattice with complete coherence. In the next two paragraphs we review two experiments that cast doubts on this physical picture.

The doping experiment reported by Iga *et al.* shows that the formation of an energy gap in the electron spectrum is not connected with coherence.^{2,9} The authors measured the magnetic susceptibility of $\text{Yb}_x\text{Lu}_{1-x}\text{B}_{12}$ for $1 \geq x > 1/32$ in the temperature range $4.2 < T < 300$ K. Using the position of the susceptibility peak as a measure of the energy gap, one can see that the alloys with $1 > x > 1/2$, all n -type semiconductors, have substantially the same energy gap as the pure material. Thus, the gap persists even though coherence is clearly not maintained for such a large range of doping. For $x < 1/2$ the alloys behave like classic Kondo systems.

The present author pointed out in a recent paper that the hybridization gap picture is also in disagreement with the inelastic neutron scattering data for another insulating compound, $\text{Ce}_3\text{Bi}_4\text{Pt}_3$.¹⁰ The hybridization gap is known to be an

indirect gap, i.e., a gap between the lower band at the Brillouin zone boundary and the upper band at the zone center. Accordingly, just as in heavy fermion materials, inelastic neutron magnetic scattering should be prominent at large scattering angles.¹¹ In contrast, Severing and co-workers observed the gap at small scattering angles.^{12,13} At sufficiently large momentum transfer the magnetic scattering actually disappears. The entire finding is at odds with the band hybridization scenario.

Inelastic neutron scattering results for YbB_{12} are more complicated but shed crucial light on the physics.^{14–16} In Ref. 14 Nefedova *et al.* reported neutron time-of-flight experiments on a powder sample at four temperatures ranging from 15 to 159 K. The spectrum was found to change drastically. At 15 K they found three peaks at 15, 20, and 38 meV. At 55 K the middle peak no longer stands out. A single-peak broad feature was seen at still higher temperatures. The polycrystalline data reported by Bouvet *et al.* are quite similar.¹⁵ The experiment reported by Iga *et al.*¹⁶ was done on a single crystal at 1.5 K. The two low energy peaks observed in Ref. 14 at low temperatures come from a band of inelastic excitations. The high energy peak at 38 meV is associated with another band. Both bands are weakly dispersive and have sizable intrinsic linewidths. These results are not explained by the existing theory for spin fluctuation in metals.

We propose in this paper that, in analogy with $\text{Ce}_3\text{Bi}_4\text{Pt}_3$, the ground state of YbB_{12} consists of a lattice of localized spin singlet superpositions of f^{14} and $f^{13}d^1$ configurations of Yb. In Sec. II we develop the formal theory under some simplifying approximations. The gap in the f electron system originates from local effects and tends to persist in incoherent systems. In a coherent periodic lattice the gap has a dispersion, in qualitative agreement with the single-crystal neutron scattering experiment.¹⁶ The theory follows the same line as the spin-fluctuation theory for metals except for differences in mathematical details necessitated by the insulating state. Section III shows how physical details are added to obtain a phenomenological theory for the bulk properties of the real material. Application of the theory to thermodynamic, magnetic, and neutron scattering experiments is discussed.

II. THEORY

The model assumes that the ground state of the material is a lattice of Yb such that the configurations f^{14} and $f^{13}d^1$ are nearly degenerate. The two $6s$ electrons of Yb form stable chemical bonds with neighboring B atoms. In the Hamiltonian we include only f electrons in atomic orbitals and d electrons in band states.

Both f^{13} and f^{14} states involve atomic orbitals of high complexity. To make the theory tractable, we first simplify the model by ignoring the orbital degeneracy, i.e., regarding the filled shell as f^2 and the one hole state as f^1 . The orbital effects will be appended later. We can then set up the model Hamiltonian as

$$\begin{aligned}
H = & \sum_{\vec{k}\sigma} \epsilon_k c_{\vec{k}\sigma}^\dagger c_{\vec{k}\sigma} + \sum_{j\sigma} \epsilon_f f_{j\sigma}^\dagger f_{j\sigma} \\
& + \frac{1}{\sqrt{N}} \sum_{\vec{k},\sigma} (V_{\vec{k}} f_{j\sigma}^\dagger c_{\vec{k}\sigma} e^{i\vec{k}\cdot\vec{R}_j} + \text{H.c.}) \\
& + U_{ff} \sum_j f_{j+}^\dagger f_{j+} f_{j-}^\dagger f_{j-}, \quad (1)
\end{aligned}$$

where \vec{R}_j is the position of the f site labeled by j . The proposed trial wave function for the local spin singlet state at the site j is

$$|\Phi_j\rangle = \left[a f_{j+}^\dagger f_{j-}^\dagger + \sum_{\vec{k}\sigma} b_{\vec{k}} f_{j\sigma}^\dagger c_{\vec{k},-\sigma}^\dagger e^{-i\vec{k}\cdot\vec{R}_j} \right] |0\rangle, \quad (2)$$

where $|0\rangle$ is the vacuum state. The relation $H|\Phi_j\rangle = E_0|\Phi_j\rangle$, where E_0 is the ground state energy, yields

$$a(2\epsilon_f + U_{ff} - E_0) + 2 \sum_{\vec{k}} b_{\vec{k}} \frac{V_{\vec{k}}}{\sqrt{N}} = 0, \quad (3)$$

and

$$b_{\vec{k}}(\epsilon_f + \epsilon_k - E_0) + a \frac{V_{\vec{k}}^*}{\sqrt{N}} = 0. \quad (4)$$

Solving Eq. (4) for $b_{\vec{k}}$ and putting the result into Eq. (3), we obtain the following equation for E_0 :

$$2\epsilon_f + U_{ff} - E_0 = \frac{1}{N} \sum_{\vec{k}} \frac{2|V_{\vec{k}}|^2}{\epsilon_f + \epsilon_k - E_0}. \quad (5)$$

The sum on \vec{k} is carried over all unoccupied parts of the band. To gain insight, we assume an empty d band extending from $\epsilon_{\vec{k}}=0$ to W with a uniform density of states ρ_0 . Equation (5) reduces to

$$E_0 = \epsilon_f - W \exp\left[-\frac{2\epsilon_f + U_{ff} - E_0}{2\rho_0 V^2}\right], \quad (6)$$

where V denotes the average matrix element. We assume in the model that the one hole state is highly stable, i.e., ϵ_f

$\ll 0$, but the filled f shell state is nearly degenerate with the f hole plus one d electron in the band, i.e., $\epsilon_f + U_{ff} \approx \epsilon_k$. Let $\epsilon_f - E_0 = \epsilon_0$; we find

$$\epsilon_0 = W \exp\left[-\frac{\epsilon_f + U_{ff} + \epsilon_0}{2\rho_0 V^2}\right]. \quad (7)$$

This equation determines ϵ_0 , which plays the role of the energy gap.

To find the wave function we solve for $b_{\vec{k}}$ in terms of a :

$$b_{\vec{k}} = -a \frac{V_{\vec{k}}}{\sqrt{N}} \frac{1}{\epsilon_0 + \epsilon_k}. \quad (8)$$

Normalization of the wave function requires $a^2 + 2 \sum_{\vec{k}} |b_{\vec{k}}|^2 = 1$. From this we find

$$a^{-2} = 1 + \frac{2\rho_0 V^2}{\epsilon_0}. \quad (9)$$

Usually the second term dominates, and the quantity $1 - a^2 \approx 1$ is the number of f holes per site.

More information on the f electron distribution can be obtained from its spectral function. We define the f electron Green's function by

$$G_f(t) = -i \langle \Phi_j | T e^{iHt} f_{j\sigma} e^{-iHt} f_{j\sigma}^\dagger | \Phi_j \rangle, \quad (10)$$

where T is the time ordering operator. The evaluation of $G_f(t)$ is straightforward:

$$\begin{aligned}
G_f(t) = & -i \sum_{\vec{k}} b_{\vec{k}}^2 e^{-i(\epsilon_f + U_{ff} + \epsilon_k + \epsilon_0)t} \theta(t) \\
& + i \left[a^2 e^{i\epsilon_0 t} + \sum_{\vec{k}} b_{\vec{k}}^2 e^{i(-\epsilon_f + \epsilon_0 + \epsilon_k)t} \right] \theta(-t),
\end{aligned}$$

where $\theta(t)$ is the step function. The Fourier transform is

$$\begin{aligned}
G_f(\omega) = & \sum_{\vec{k}} \frac{b_{\vec{k}}^2}{\omega - \epsilon_0 - \epsilon_f - U_{ff} - \epsilon_k - i\delta} \\
& + \frac{a^2}{\omega + \epsilon_0 + i\delta} + \sum_{\vec{k}} \frac{b_{\vec{k}}^2}{\omega - \epsilon_f + \epsilon_0 + \epsilon_k + i\delta}.
\end{aligned}$$

From this we calculate the density of states,

$$\begin{aligned}
\rho_f(\omega) = & a^2 \delta(\omega + \epsilon_0) + \sum_{\vec{k}} b_{\vec{k}}^2 \delta(\omega - \epsilon_f + \epsilon_0 + \epsilon_k) \\
& + \sum_{\vec{k}} b_{\vec{k}}^2 \delta(\omega - \epsilon_0 - \epsilon_f - U_{ff} - \epsilon_k).
\end{aligned}$$

Converting the sum into an integral over band energies, we obtain

$$\rho_f(\omega) = a^2 \delta(\omega + \epsilon_0) + \frac{1}{2\pi} \frac{\gamma}{(\omega - \epsilon_f + \epsilon_0)^2} + \frac{1}{2\pi} \frac{\gamma}{(\omega - \epsilon_0 - \epsilon_f - U_{ff})^2},$$

where $\gamma = 2\pi a^2 \rho_0 V^2$. The divergences in the last two terms are rounded off by the f level width, so

$$\rho_f(\omega) = a^2 \delta(\omega + \epsilon_0) + \frac{1}{2\pi} \frac{\gamma}{(\omega - \epsilon_f + \epsilon_0)^2 + \gamma^2} + \frac{1}{2\pi} \frac{\gamma}{(\omega - \epsilon_0 - \epsilon_f - U_{ff})^2 + \gamma^2}. \quad (11)$$

The f level width is $\gamma \approx \pi \epsilon_0$. Equation (11) is the well-known multiple peak structure for the f electron distribution obtained for metals.⁵ The only difference is that the level at $-\epsilon_0$ is below the band. The peak at $\epsilon_f - \epsilon_0$ is inconsequential for our purpose, but the one at $\epsilon_0 + \epsilon_f + U_{ff}$ will play an important role to be discussed later. The complete Green's function is

$$G_f(\omega) = \frac{a^2}{\omega + \epsilon_0 + i\delta} + \frac{1}{2} \frac{1}{\omega - \epsilon_f + \epsilon_0 + i\gamma} + \frac{1}{2} \frac{1}{\omega - \epsilon_0 - \epsilon_f - U_{ff} - i\gamma}. \quad (12)$$

In a similar manner we define the d electron Green's function by

$$G_{\vec{k}}(t) = -i \langle T e^{iHt} c_{\vec{k}\sigma}^- e^{-iHt} c_{\vec{k}\sigma}^+ \rangle, \quad (13)$$

where the expectation value is taken in the coherent ground state of the full periodic lattice. We find by taking its time derivative that

$$\left(i \frac{\partial}{\partial t} - \epsilon_k \right) G_{\vec{k}}(t) = \delta(t) - i \frac{V_{\vec{k}}^*}{\sqrt{N}} \times \sum_j \langle T e^{iHt} f_{j\sigma} e^{-iHt} c_{\vec{k},\sigma}^+ e^{-i\vec{k} \cdot \vec{R}_j} \rangle.$$

We denote the last term in the above equation by $F_{\vec{k}}(t)$. Its equation of motion is

$$\left(i \frac{\partial}{\partial t} - \epsilon_k \right) F_{\vec{k}}(t) = - \frac{V_{\vec{k}}}{\sqrt{N}} G_f(t).$$

We Fourier analyze the equations and solve for $G_{\vec{k}}(\omega)$ to obtain

$$G_{\vec{k}}(\omega) = \frac{1}{\omega - \epsilon_k} + \frac{V^2 G_f(\omega)}{(\omega - \epsilon_k)^2}.$$

This result can be recognized as the leading terms of a Dyson series, which can be summed up to yield

$$G_{\vec{k}}(\omega) = [\omega - \epsilon_k - V^2 G_f(\omega)]^{-1}. \quad (14)$$

In the neighborhood of $\omega=0$, Eqs. (12) and (14) give the dispersion relation for a band of quasiparticles, commonly known as slave bosons:

$$(\omega - \epsilon_k)(\omega + \epsilon_0) - a^2 V^2 = 0. \quad (15)$$

Since the level $-\epsilon_0$ does not cross the band, the hybridization interaction merely gives the slave boson band a slight shift and dispersion. No new gap is created. In the neighborhood of the one f hole state $\omega = \epsilon_f + U_{ff}$, the band dispersion is solved from

$$(\omega - \epsilon_k)(\omega - \epsilon_0 - \epsilon_f - U_{ff} - i\gamma) - \frac{1}{2} V^2 = 0. \quad (16)$$

This upper band has both dispersion and damping.

Another important result that can be derived within this framework is the static susceptibility. We apply a magnetic field B to the system. The Hamiltonian is

$$H = \sum_{\vec{k}\sigma} (\epsilon_k - \mu_B B \sigma) c_{\vec{k}\sigma}^\dagger c_{\vec{k}\sigma} + \sum_{j\sigma} (\epsilon_f - \mu_f B \sigma) f_{j\sigma}^\dagger f_{j\sigma} + \frac{1}{\sqrt{N}} \sum_{\vec{k},\sigma} (V_{\vec{k}} f_{j\sigma}^\dagger c_{\vec{k}\sigma} e^{i\vec{k} \cdot \vec{R}_j} + \text{H.c.}) + U_{ff} \sum_j f_{j+}^\dagger f_{j+} f_{j-}^\dagger f_{j-},$$

where μ_f is the effective moment of Yb,¹³ and μ_B is the moment for the d electron. The following field dependent variational wave function is used to calculate the ground state energy:

$$|\Phi_j\rangle = \left(a f_{j+}^\dagger f_{j-}^\dagger + \sum_{\vec{k}\sigma} b_{\vec{k}\sigma} f_{j\sigma}^\dagger c_{\vec{k},-\sigma}^\dagger \right) |0\rangle.$$

Without repeating the same algebra, we write down the equation for E_0 :

$$2\epsilon_f + U_{ff} - E_0 = \frac{1}{N} \sum_{\vec{k}} \left[\frac{|V_{\vec{k}}|^2}{\epsilon_f + \epsilon_k - E_0 - (\mu_f - \mu_B)B} + \frac{|V_{\vec{k}}|^2}{\epsilon_f + \epsilon_k - E_0 + (\mu_f - \mu_B)B} \right].$$

For the simple band with uniform density of states ρ_0 ,

$$2\epsilon_f + U_{ff} - E_0 = \rho_0 V^2 \left[\ln \frac{W}{\epsilon_f - E_0 - (\mu_f - \mu_B)B} + \ln \frac{W}{\epsilon_f - E_0 + (\mu_f - \mu_B)B} \right] \approx 2\rho_0 V^2 \ln \frac{W}{\epsilon_f - E_0} + 2\rho_0 V^2 B^2 \frac{(\mu_f - \mu_B)^2}{(\epsilon_f - E_0)^2}.$$

For sufficiently weak hybridization the solution is

$$\epsilon_0(B) = \epsilon_0 - B^2 \frac{(\mu_f - \mu_B)^2}{\epsilon_0}.$$

The ground state susceptibility is obtained by differentiation,

$$\chi_0 = \frac{2(\mu_f - \mu_B)^2}{\epsilon_0}. \quad (17)$$

The result has the form of the Van Vleck susceptibility of a two level system separated by energy ϵ_0 . The effective moment $\mu_f - \mu_B$ is much reduced from both μ_f and μ_B .

We summarize this section by emphasizing that the dynamics of the f electrons is treated locally, which is a good approximation considering the tightness of the $4f$ wave function. The d electron states are treated according to the periodic Anderson model with full coherence. In an incoherent system, such as Lu doped samples, the f electron spectrum continues to hold but the d electron effects in Eqs. (15) and (16) are no longer valid. Since the latter effects make only subtle changes to the f electron spectrum, the theory concludes that the gap is a local property and persists in systems where the Yb sites are partly replaced with Lu.

III. PHENOMENOLOGICAL MODEL FOR BULK PROPERTIES

The model in the last section, while sufficient to establish an insulating ground state and a band of excited states, ignores a number of details which become important when we make comparisons with experiments. Due to spin-orbit degeneracy, the filled $4f$ shell of Yb is a complex atomic state involving 14 electrons. The one hole state for Yb has eight sublevels. As a result, the actual trial wave function for the ground state must contain one f^{14} term and eight $f^{13}d^1$ terms. The ground state should remain nondegenerate and nonmagnetic. The excited states, however, are a set of eight one hole f levels hybridized with the d band. The crystal field will split the f levels to give more structure to the neutron scattering signal. The d band usually has many branches, which put the determination of the hybridized bands beyond the scope of the model.

In this section we propose a phenomenological model for the bulk properties of the material based on the findings of the microscopic theory. It contains some of the complexity of the real material, but one can choose a small set of model parameters to fit a considerable amount of bulk data.

Consider an insulator with a filled valence band denoted by $\epsilon_{1\vec{k}}$ and an empty conduction band $\epsilon_{2\vec{k}}$. The inelastic neutron scattering cross section at zero temperature is given by

$$S(\vec{q}, \omega) = \sum_{\vec{k}} \delta(\epsilon_{1\vec{k}} - \epsilon_{2, \vec{k} + \vec{q}} + \omega).$$

If the valence band is entirely flat, i.e., $\epsilon_{1\vec{k}} = \epsilon_1$, we find

$$S(\vec{q}, \omega) = \rho_2(\epsilon_1 + \omega),$$

where $\rho_2(\epsilon)$ is the density of states of the conduction band. The neutron signal has no \vec{q} dependence, and its linewidth

reflects the dispersion of the conduction band. Any \vec{q} dependence of the neutron scattering line implies that the valence band also has a dispersion, such as that obtained from the microscopic model in Sec. II.

For bulk properties we propose to ignore the valence band dispersion and treat the ground state as a sharp, local level at $-\epsilon_0$. Neutron scattering experiments show that the excited states consist of two sets of narrow bands formed by d - f hybridization.¹⁴⁻¹⁶ We denote the density of states of the two hybridized bands by $\rho_i(\epsilon)$ with $i=1,2$. The experiments do not reveal how many sublevels there are in each band, but we will show that, by assigning fourfold degeneracy to each band, we obtain the best fit to the bulk data. In principle, both ϵ_0 and the bands are temperature dependent. Unlike in the metal problem, however, the Fermi level in the insulator does not intersect the band to cause a sensitive temperature effect at low temperatures. Accordingly, we ignore the temperature dependence of ϵ_0 and $\rho_i(\epsilon)$ and determine the Fermi level μ by the conservation of particles:

$$1 = f(-\epsilon_0) + \sum_{i=1,2} \int \rho_i(\epsilon) f(\epsilon) d\epsilon, \quad (18)$$

where $f(\epsilon) = 1/[e^{\beta(\epsilon - \mu)} + 1]$. The internal energy $E(T)$ is given by

$$E(T) = -\epsilon_0 f(-\epsilon_0) + \sum_{i=1,2} \int \rho_i(\epsilon) \epsilon f(\epsilon) d\epsilon. \quad (19)$$

The specific heat is calculated from $C(T) = dE(T)/dT$. As shown in Ref. 14, the density of states of the lower band can be approximated by a double Lorentzian,

$$\rho_1(\omega) = \frac{g_1}{2\pi} \left[\frac{\Gamma_1}{(\omega - E_1)^2 + \Gamma_1^2} + \frac{\Gamma_2}{(\omega - E_2)^2 + \Gamma_2^2} \right], \quad (20)$$

while the upper band can be represented by a single Lorentzian,

$$\rho_2(\omega) = \frac{g_2}{\pi} \frac{\Gamma_3}{(\omega - E_3)^2 + \Gamma_3^2}. \quad (21)$$

The parameters are taken from Ref. 14 as $E_1 = 15$ meV, $E_2 = 20$ meV, $E_3 = 40$ meV, $\Gamma_1 = 3.5$ meV, $\Gamma_2 = 5$ meV, and $\Gamma_3 = 15$ meV. All energy levels are measured from the ground state. The degeneracy numbers are taken as $g_1 = g_2 = 4$. The specific heat calculated with these parameters is compared with experimental data in Fig. 1. The theoretical curve is quite close to the older data of Kasuya *et al.*,¹ but considerably higher than the more recent data published by the same group.² By choosing $g_1 = 2$ we can fit the peak of the specific heat data in Ref. 2, but the theoretical curve is much too broad compared with the experiment.

The magnetic susceptibility consists of three parts, the Van Vleck term, the Pauli term, and the Curie term. The Van Vleck term is

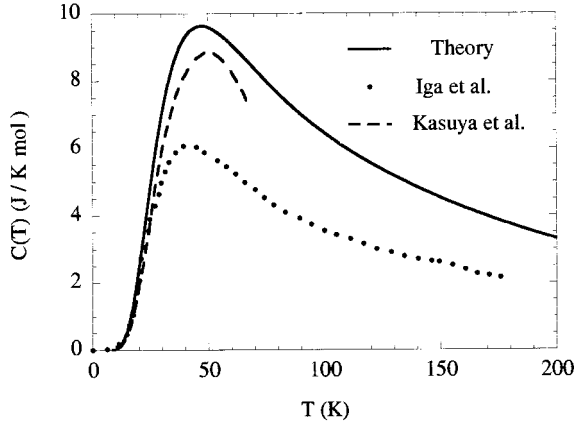


FIG. 1. The specific heat calculated from the model for bulk properties (solid curve) compared with experiments. The theory agrees well with the data published by Kasuya *et al.* (Ref. 1) and not as well with the more recent data published by the same group (circles) (Ref. 2).

$$\chi_{vv} = \sum_{i=1,2} \mu_i^2 \int \frac{f(-\epsilon_0) - f(\epsilon)}{\epsilon + \epsilon_0} \rho_i(\epsilon) d\epsilon + \mu_{12}^2 \int \int \frac{f(\epsilon) - f(\epsilon')}{\epsilon - \epsilon'} \rho_1(\epsilon) \rho_2(\epsilon') d\epsilon d\epsilon'. \quad (22)$$

The quantities μ_i and μ_{12} are the effective orbital moments. The first term arises from virtual transitions from the ground state to the two bands and the last term comes from transitions between the two bands, which are important only at elevated temperatures when the lower band is sufficiently occupied. When the ground state is broken up by thermal excitation, the d electron moves into the bands and leaves behind a free Yb^{3+} core. The electrons in the bands contribute to a Pauli susceptibility

$$\chi_p = \frac{\mu_p^2}{T} \sum_{i=1,2} \int f(\epsilon) [1 - f(\epsilon)] \rho_i(\epsilon) d\epsilon, \quad (23)$$

where μ_p is the effective magnetic moment of the band electrons. The localized magnetic moments of Yb^{3+} contribute to a Curie susceptibility

$$\chi_c = \frac{\mu_c^2 [1 - f(\epsilon_0)]}{T}, \quad (24)$$

where μ_c is the moment of the one f hole state. The magnetic moment of Yb^{3+} is $\mu_f = g \mu_B \sqrt{j(j+1)}/3 = 2.62 \mu_B$. Therefore, the theoretical values of these magnetic moment parameters are $\mu_1 = \mu_2 = \mu_f - \mu_B = 1.62 \mu_B$, $\mu_{12} \approx \mu_1$, $\mu_p \approx \mu_B$, and $\mu_c \approx \mu_f$. In Fig. 2 we show a fit of the theory to the data using the parameters $\mu_1 = \mu_2 = 0.5 \mu_B$, $\mu_{12} = 0.2 \mu_B$, $\mu_p = \mu_B$, and $\mu_c = 1.3 \mu_B$. Some of these effective moments are considerably smaller than the theoretical values, probably due to hybridization, the crystal field, and other unknown effects. Also plotted on the same graph are static susceptibility data as deduced from inelastic neutron scattering.¹⁴ The neutron data do not agree with the bulk data at low tempera-

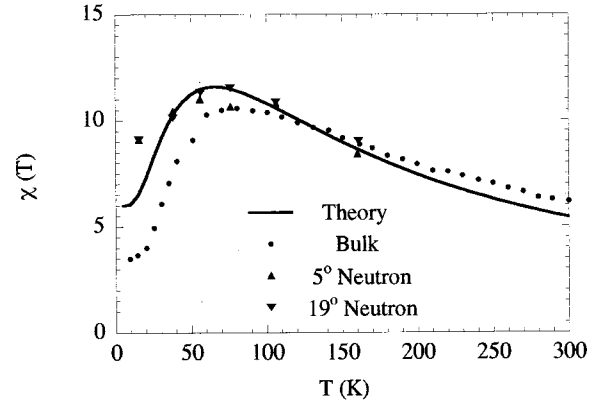


FIG. 2. The calculated magnetic susceptibility (solid curve) compared with the bulk data (circles) (Ref. 2) and results extracted from inelastic neutron scattering (triangles). (Ref. 14) A possible reason for the discrepancy between bulk and neutron data is discussed in the text.

tures, and the theoretical curve agrees better with the neutron data. A possible source of discrepancy will be discussed after the next paragraph.

The inelastic neutron scattering cross section for the polycrystal also has three terms. The Van Vleck term is

$$\chi''_{vv}(\omega) = \sum_{i=1,2} \mu_i^2 [f(\epsilon_0) - f(\epsilon_0 + \omega)] \rho_i(\epsilon_0 + \omega) + \mu_{12}^2 \int [f(\epsilon) - f(\epsilon + \omega)] \rho_1(\epsilon) \rho_2(\epsilon + \omega) d\epsilon. \quad (25)$$

The Pauli and Curie terms together give rise to the spin diffusion term, which is approximated by

$$\chi''_d(\omega) = (\chi_p + \chi_c) \frac{\omega}{\sqrt{\pi} \Gamma_c} \exp\left(-\frac{\omega^2}{\Gamma_c^2}\right). \quad (26)$$

The total scattering cross section is

$$S(\omega) \propto \frac{\chi''(\omega)}{1 - e^{-\beta\omega}}, \quad (27)$$

where $\chi''(\omega) = \chi''_{vv}(\omega) + \chi''_d(\omega)$. We find that the Gaussian form for the spin diffusion contribution gives a more satisfactory fit to the data than the Lorentzian form. The diffusion constant $\Gamma_c \propto \sqrt{T}$ adds one more parameter to the theory. The four panels in Fig. 3 show the fit to the data in Ref. 14 at four temperatures. Aside from one vertical scale which applies at all temperatures the only fitting parameter is $\Gamma_c = \sqrt{2T}$ in meV, where T is measured in K. The theory predicts correctly the variation of the neutron line shape as a function of temperature. In particular, at high temperatures the broad peak at 20 meV is largely due to transitions between the two quasi particle bands.

One can deduce the static susceptibility from inelastic neutron scattering as discussed in Ref. 14. The procedure relies on an extrapolation to zero momentum transfer by us-

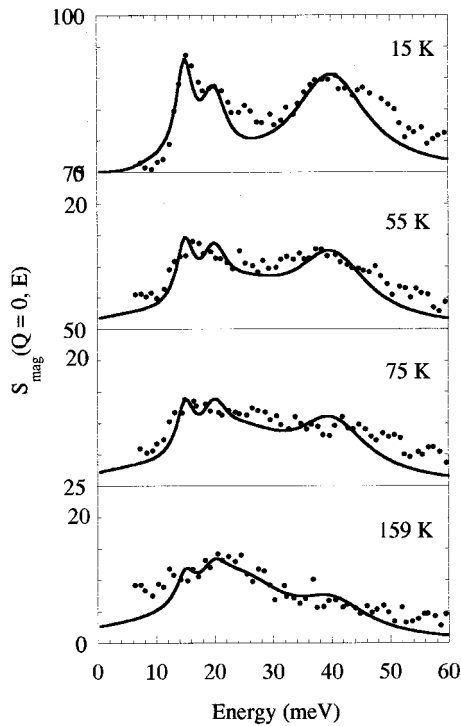


FIG. 3. Comparison of calculated inelastic scattering cross section at four temperatures (solid curves) with the data in Ref. 14 (circles).

ing the $4f$ form factor for Yb.¹³ Here may lie the source of disagreement with the bulk data. As shown in Eq. (17), the bulk susceptibility contains a d contribution that has the opposite sign from the f contribution. The $5d$ electron has a narrower form factor than $4f$, so an extrapolation based on the $4f$ form factor may be unreliable. The theory seems to agree better with the neutron data, implying that the phenomenological model, which takes its input from neutron scattering data, is self-consistent. A powerful test of both the mi-

croscopic theory and the bulk model would be a measurement of the neutron magnetic form factor of this interesting material.

IV. DISCUSSION

The Lu doping experiments reported by Iga and co-workers lend further support to our proposed ground state, i.e., a lattice of localized singlet bound states involving Yb^{2+} and $\text{Yb}^{3+}d^1$.^{2,9} The Lu doped samples have negative Hall mobility.⁹ Our interpretation of this effect is that Lu already has a filled $4f$ shell, so no bound state can form on its site. This puts the d electrons of Lu in the band as charge carriers. The observed gaps in the susceptibility data are local gaps on Yb sites. Neutron scattering experiments are under way to verify this prediction.¹⁷

It is particularly interesting to contrast the doping behavior of YbB_{12} and $\text{Ce}_3\text{Bi}_4\text{Pt}_3$. A simple rule relates the electron number of the dopant to the carrier charge in semiconductors. The dopant Lu has one more electron than the host Yb, so the extra electron becomes the free carrier as expected from the rule. The rule is violated in the Ce compound because when it is doped with La, which has one fewer electron than Ce, the alloy is an n -type semiconductor.¹⁸ We suggest that the difference in the doping behavior of the two compounds arises from an important difference in their ground states, i.e., the ground state of the Yb system may be regarded as a lattice of bound states of an f hole with a d electron, but for the Ce system the ground state consists of local bound states of an f electron and a d electron on Ce sites.¹⁰

ACKNOWLEDGMENTS

The author is indebted to Professor P. A. Alekseev for suggesting the investigation and for his guidance through the massive amount of literature. He also wishes to thank Professor B. Maple and Professor L. J. Sham of the University of California, San Diego for their hospitality.

- ¹M. Kasuya, F. Iga, M. Takigawa, and T. Kasuya, *J. Magn. Magn. Mater.* **47&48**, 429 (1985), and references cited therein.
- ²F. Iga, S. Hiura, J. Klijn, N. Shimizu, T. Takabatake, M. Ito, Y. Matsumoto, F. Masaki, T. Suzuki, and T. Fujita, *Physica B* **259-261**, 312 (1999), and references cited therein.
- ³Z. Fisk *et al.*, *Physica B* **206&207**, 798 (1995).
- ⁴C.M. Varma and Y. Yafet, *Phys. Rev. B* **13**, 2950 (1976).
- ⁵N.E. Bickers, D.L. Cox, and J.W. Wilkins, *Phys. Rev. Lett.* **54**, 230 (1985); *Phys. Rev. B* **36**, 2036 (1987).
- ⁶A. Auerbach and K. Levin, *Phys. Rev. Lett.* **57**, 877 (1986); *Phys. Rev. B* **34**, 3524 (1986).
- ⁷A.J. Millis and P.A. Lee, *Phys. Rev. B* **35**, 3394 (1987).
- ⁸J.-M. Duan, D.P. Arovas, and L.J. Sham, *Phys. Rev. Lett.* **79**, 2097 (1997).
- ⁹F. Iga, M. Kasuya, and T. Kasuya, *J. Magn. Magn. Mater.* **52**, 312 (1985).
- ¹⁰S.H. Liu, *Phys. Rev. B* **60**, 13 429 (1999).
- ¹¹G.H. Kwei, J.M. Lawrence, P.C. Canfield, W.P. Beyermann, J.D. Thompson, Z. Fisk, A.C. Lawton, and A.J. Goldstone, *Phys. Rev. B* **46**, 8067 (1992).
- ¹²A. Severing, J.D. Thompson, P.C. Canfield, Z. Fisk, and P. Riseborough, *Phys. Rev. B* **44**, 6832 (1991).
- ¹³A. Severing, J.D. Thompson, P.C. Canfield, Z. Fisk, and P. Riseborough, *J. Alloys Compd.* **181**, 217 (1992).
- ¹⁴E.V. Nefeodova, P.A. Alekseev, J.-M. Mignot, V.N. Lazukov, I.P. Sadikov, Yu.B. Paderno, N.Yu. Shitsevalova, and R.S. Eccleston, *Phys. Rev. B* **60**, 13 507 (1999).
- ¹⁵A. Bouvet, T. Kasuya, M. Bonnet, L.P. Regnault, J. Rossat-Mignod, F. Iga, B. Fåk, and A. Severing, *J. Phys.: Condens. Matter* **10**, 5667 (1998).
- ¹⁶F. Iga, A. Bouvet, L.P. Regnault, T. Takabatake, A. Hiess, and T. Kasuya, *J. Phys. Chem. Solids* **60**, 1193 (1999).
- ¹⁷P. A. Alekseev (private communication).
- ¹⁸P.C. Canfield, J.D. Thompson, Z. Fisk, M.F. Hundley, and A. Lucerda, *J. Magn. Magn. Mater.* **108**, 217 (1992).